MAGNETIC RESONANCE IN CHEMISTRY
Magn. Reson. Chem. **36**, S29–S43 (1998)

Analysis of substituent effects on ^{31}P NMR chemical shifts: PX_2Y molecules†

Alk Dransfeld and Paul von Ragué Schleyer*

Institut für Organische Chemie der Universität Erlangen-Nürnberg, Henkestrasse 42, 91054 Erlangen, Germany

Received 18 September 1997; accepted 29 November 1997

ABSTRACT: Tricoordinate phosphorus NMR chemical shifts are computed (GIAO/6–311 + G**//RMP2(fc)/6–31 + G*) and analyzed for PX_2Y molecules (X, Y = EH_n: F, OH, NH_2, CH_3, BH_2, BeH, Li and H = 'simple first row substituents'), the 'normal' $\delta(^{31}P)$ relationship with the substituent electronegativity sum, $\sum EN$ ($\sum_{i=1}^{3} EN(E_i)$; downfield shift with increasing $\sum EN$) is substantiated for experimentally important molecules by the *ab initio* results. The 'inverse' $\delta(^{31}P)$–$\sum EN$ trend obtained for X = F is related to negative hyperconjugation ($Lp(X) \rightarrow \sigma^*$ (P—X′) orbital interaction). The $P(OH)_2Y$ molecules display 'normal' $\sum EN$–shift relationships when the electronegativity of Y is low and 'inverse' when the electronegativity of Y is high. For some PX_2Y phosphanes with simple substituents, the $\delta(^{31}P)$ values are well related to $\sum EN$. The best correlation (cc: 0.955) between $\delta(^{31}P)$ and $\sum EN$ is found for the set of monosubstituted phosphanes, PH_2X. The $\delta(^{31}P)$–EN(Y) slope (in ppm per EN 'unit'), ranges from 162 (X = BeH), 141 (X = H) and 98 (X = CH_3 and X = BH_2) to −105 (X = F). The $\delta(^{31}P)$ values of the PX_2Y molecules are representative for the complete set of PXYZ with simple substituents. Since there is no 'simple, general relationship' of $\delta(^{31}P)$ for phosphanes with less or much more electronegative substituents, $EN(E) < EN(P) \ll EN(E)$, consequently, it does not exist in the complete set. © 1998 John Wiley & Sons, Ltd.

KEYWORDS: NMR; ^{31}P NMR; ^{31}P chemical shifts; GIAO/6–311 + G** MP2 geometries; tricoordinate phosphorus; negative hyperconjugation; electronegativity

INTRODUCTION

Substituents on tricoordinate phosphorus induce exceptionally large changes in the ^{31}P NMR chemical shifts (ranging over 500 ppm).[1–5] Early attempts to systematize this behavior have employed increments for each type of substituent (see, e.g., Table 1).[1–3,6,7] For example, such procedures work reasonably well for ^{13}C NMR shifts of methane derivatives (substituents: H, alkyl, alkoxy or an amino group), where the errors in ^{13}C shift estimates are less than 10 ppm for a range of about 100 ppm.[7,8] In contrast, shift increment treatments for $\delta(^{31}P)$ result in larger errors[9] (70 ppm; range over 500 ppm). The performance of experimentally derived increments (Table 1) is illustrated by the $\delta_{est}(^{31}P)$–$\delta_{exp}(^{31}P)$ plot (Fig. 1). While many of the points are close to the solid line (exact match of estimate and experiment), the majority are found in the '70 ppm area' (between the solid and the dotted line) and only a few deviate by as much as 217 ppm. What is responsible for the deviations? Are increments inappropriate to describe substituent effects on $\delta(^{31}P)$ when more than one highly electronegative group is present (e.g. due to mutual interaction)?

Table 1. Selected NMR shift increments (ppm) for ^{13}C (tetracoordinate carbon)[a] and ^{31}P (tricoordinate phosphorus)[b]

	X = H	X = R[c]	X = NR_2[c]	X = OR[c]	X = F	X = Cl	rmse
^{13}C[a]	0	9	28	58	70	31	10
^{31}P[b]	−69	−20[d]	47	55	25	74	70

[a] The $\delta(^{13}C)$ increments are with respect to CH_4, $\delta(^{13}C) = -2$ (see Ref. 67).
[b] The $\delta(^{31}P)$ increments are with respect to PPh_3, $\delta(^{31}P) = -7$ (see Refs 1 and 2).
[c] R = alkyl.[24,67]

Is the influence of the substituent, Y, on the chemical shift of the central atom constant, as assumed in increment system treatments? The localized[10] molecular orbitals employed in the IGLO method[11] allow contributions of bonds, lone pairs, etc., to the isotropic magnetic shielding to be assigned (e.g. to P—X and P—Y). IGLO results[11] for the $PH_{3-n}F_n$ (Table 2) and the $SiH_{4-n}F_n$ set provided contributions to $\delta(^{31}P)$ from the P—F molecular orbitals, $\Delta\delta_{IGLO}(^{31}P(P—F))$. The Si—F bond 'shift increments,' $\Delta\delta_{IGLO}(^{29}Si(Si—F))$, for $SiH_{4-n}F_n$ (−63, −71, −76 and −78 for $n = 1$ to 4) range over only 15 ppm. In contrast, variation of the P—F bond 'shift increments,' $\Delta\delta_{IGLO}(^{31}P(P—F))$, in $PH_{3-n}F_n$ are −61, −84 and −104 ppm for $n = 1$ to 3. The range of $\Delta\delta_{IGLO}(^{31}P(P—F))$ values (43 ppm) is nearly three times larger than the Si—F bond 'shift

* Correspondence to: P. v. R. Schleyer, Institut für Organische Chemie der Universität Erlangen-Nürnberg, Henkestrasse 42, 91054 Erlangen, Germany. E-mail address: schleyer@organik.uni-erlangen.de
† Dedicated to Professor John D. Roberts on the occasion of his 80th birthday.
Contract/grant sponsor: Deutsche Forschungsgemeinschaft.

 CCC 0749-1581/98/SI0029–15 $17.50

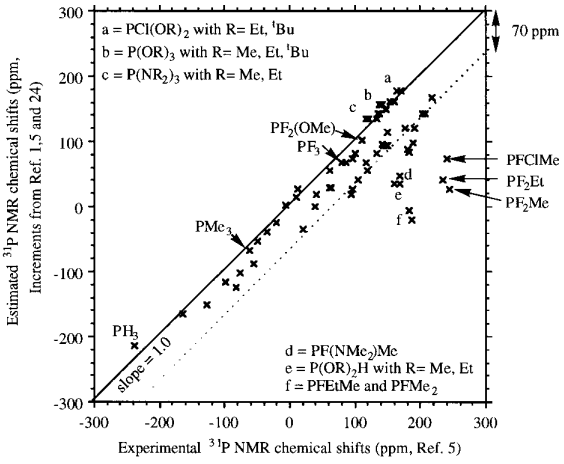

Figure 1. Experimental (Ref. 5) and estimated (increment system based on Refs 1, 5 and 24) ^{31}P NMR chemical shifts for PXYZ with X, Y, Z = H, CH_3, NH_2, F, Et, ^{i}Pr, ^{t}Bu, NMe_2, NEt_2, N^tBu_2, OMe, O^{i}Pr and O^{t}Bu (rmse = 69 ppm; see supplementary material). The errors of estimates for alkyl-substituted phosphanes can be reduced from a maximum deviation of −128 ppm to a range between −42 and 25 ppm by differentiation between Me, Et, ^{i}Pr and ^{t}Bu (Ref. 24).

increment' range. This emphasizes the greater difficulties to be expected in increment treatment for $\delta(^{31}P)$ compared with $\delta(^{29}Si)$.

Which effects influence $\delta(^{31}P)$s in general?

Substituents induce a deformation of the atom orbitals (e.g. of the ^{31}P nucleus) and thereby change the 'effective magnetic field' (see Computational Methods) at the nucleus which is addressed as the NMR chemical shift. The deformation of the electron distribution was approximated by point charges (NAO-PC)[12] in a recent neuronal network[13] application based on semi-empirically (PM3)[14] obtained parameters.[15] The root mean square error (rmse) of the predicted versus the published $\delta(^{31}P)$ values (ranging over 700 ppm) is only 28 ppm with this approach for a set of 415 di- to penta-coordinate neutral phosphorus compounds with H, alkyl, aryl, alkoxy and amino (but no fluoro) substituents.[16] Nevertheless, none of the neuronal network descriptors[17] (number of substituents, bond order[18] sum, natural atomic orbital–point charges, NAO–PC, on phosphorus,[12] etc.) dominated.[15]

NMR shift correlations

Kutzelnigg *et al.*'s IGLO[11] calculations (Table 2) for the PH_2—Y set with X = H, CH_3, NH_2, OH and F display the 'normal' relationship of $\delta(^{31}P)$ with the sub-

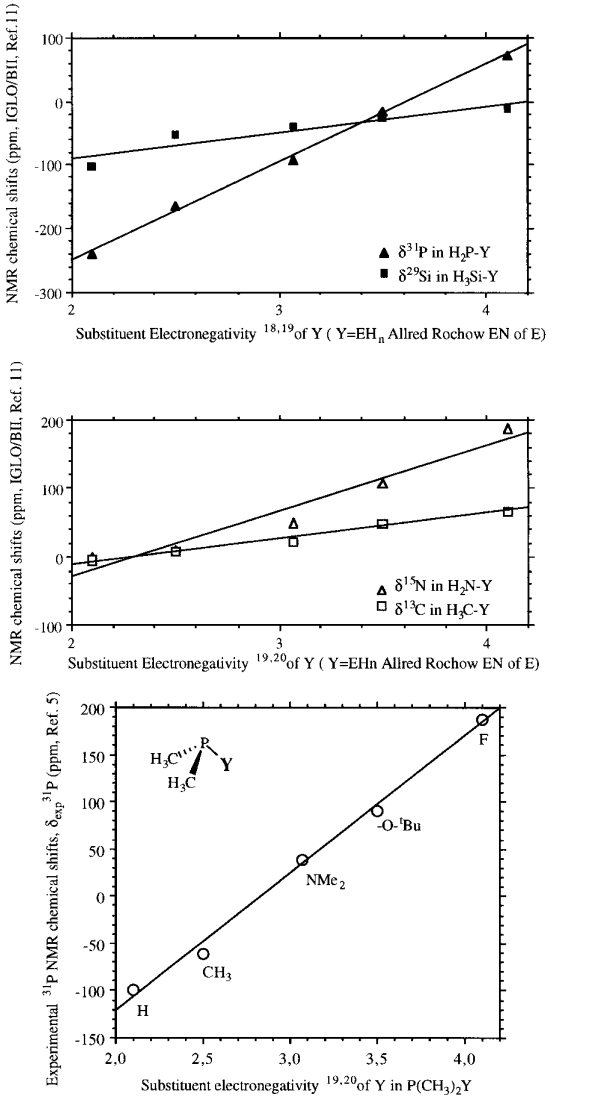

Figure 2. IGLO/BII[11]-calculated NMR chemical shifts of (a) H_3CY and H_2NY (slope 37 and 95), (b) H_3SiY and H_2PY (slope 32 and 154) with Y = H, CH_3, NH_2, OH, F versus substituent electronegativity (Allred–Rochow).[19,20] The missing value for H_3Si-NH_2 in Ref. 11 is augmented. (c) Experimental ^{31}P NMR chemical shifts, $\delta_{exp}(^{31}P)$, from Ref. 5) versus substituent electronegativity of Y (Y = EH_n, Allred–Rochow *EN* of E, Ref. 19) in $P(CH_3)_2Y$ phosphanes [$k_0 = -414$ and $k_1 = 146$ in $\delta(^{31}P) = k_0 + k_1$ *EN*(Y), Eqn (1)].

stituent electronegativity [Fig. 2(a); compare Fig. 2(c)]: the more electronegative the substituents, the more downfield are the chemical shifts. Such correlations between the substituent electronegativities[19,20] and ^{31}P NMR chemical shifts can be described by

$$\delta(^{31}P)(PX_2Y) = k_0 + k_1 EN(Y) \quad (1)$$

(where k_1 is the slope of the correlation line). Note that the $\delta(^{31}P)$ PH_2F value does not deviate significantly with respect to the correlation line [solid line in Fig. 2(a)]. The $\delta(^{31}P)$–*EN*(Y) slopes of H_2PY, $k_1(^{31}P) = 154$, and for the set of H_2NY congeners, $k_1(^{15}N) = 95$ [Fig.

Table 2. Experimental[a–f,k–q] and *ab initio*[g–k] ^{31}P NMR chemical shifts of PX_2Y phosphanes (X, Y = H, first-row substituents, numbering according to Fig. 4)

	PF_3 (1)	F_2PNH_2 (3)	F_2PMe (4)	Me_2PF (25)	PMe_3 (28)	Me_2P–H (29)
Experimental	105.66[a]			185[a]	−63.36[a]	
	97(l)[b]	147.5[c]	250.7[d]	187[e]	−62[f]	−98.5[f]
LORG '90[g]	48	…	…	…		(−135)
GIAO '91[h]	93	…	…	…	−79	…
IGLO '90[i]	83	…	197	…	−94	−127
GIAO–G94[j]	112	146	244	173	−81	−111
EMPI '96[k]	106	…	…	…	−96	−127

	PH_3 (37)	$P(CH_3)H_2$ (36)	$P(NH_2)H_2$ (35)	$P(OH)H_2$ (34)	PFH_2 (33)	H_2PLi (40)
Experimental	−266.10[a]		…	…		
	−238[f]	−163.5[f]			…	−283[l]
LORG '90[g]	−240	(−181)	…	…	…	…
GIAO '91[h]	−240	−141	…	…	…	…
IGLO '90[i]	−240	−164	−93	−16	71	…
GIAO–G94[j]	−240	−166	−84	19	95	−341[l]
EMPI '96[k]	−274	−160	…	…	…	…

	$PF_2(NMe_2)$	$PF_2(OMe)$	$P(OMe)_3$	$P(OMe)_2(NMe_2)$	$P(OMe)_2$ Me	$P(OMe)_2$ H	$P(CH_3)_2$ (OMe)	$P(CH_3)_2(NMe_2)$
Experimental	143.2[m]	111[n]	141–139.6°	148[p]	182.5[q] 200.8°	171[r]	91°	39[f]

[a] Gas-phase measurements with extrapolation to zero pressure value, Ref. 68.
[b] Ref. 69.
[c] Ref. 70.
[d] Ref. 71.
[e] Ref. 29.
[f] Ref. 1.
[g] LORG/[6s4p2d(P),3s2p1d(F)]//experimental geometry, Ref. 60; in parentheses LORG/6–311G* on optimized geometries (Me_2PH, RHF/6–31G*; $MePH_2$, RMP2(fc)/6–31G*; PH_3, RMP2(fu)/6–311 + G**).
[h] GIAO/6–311G(2d,p)//6–311G(d,p), Ref. 72.
[i] Ref. 11 in agreement with absolute shieldings for PH_3, PH_2F and PF_3 with IGLO (various basis sets and various geometries, Ref. 73).
[j] GIAO[43]/6–311 + G**//RMP2(fc)/6–31 + G** from Table 3.
[k] EMPI/tzp(H to Ne), tz2p(Na to Ar)//RMP2(fc)/6–311G(d,p), Ref. 33, isotropic shielding transformed to chemical shifts with shielding of '85% H_3PO_4, = 328.35 ppm.[68]
[l] In monoglyme, Ref. 74; deviation of the GIAO–G94[j] result with respect to the experimental value is likely to be due to the neglect of solvent effects.
[m] Ref. 75.
[n] Ref. 76.
[o] Ref. 77.
[p] Ref. 78.
[q] Ref. 79.
[r] Refs 80, 81.

2(b)], are larger than those for the tetracoordinate H_3Si—Y, $k_1(^{29}Si) = 32$ [Fig. 4(a)] and H_3C—Y, $k_1(^{13}C) = 37$ [Fig. 2(b)]. The effect of electronegativity is also illustrated by the experimentally derived ^{31}P NMR shifts of simple PMe_2Y (290 ppm range) depicted in Fig. 2(c). In their review, Maier *et al.*[21] concluded that for phosphanes 'the electronegativity of substituents on phosphorus and the angles between them are the two most important variables determining ^{31}P chemical shifts.'

A bond angle–chemical shift relationship has been found in cyclooligophosphanes, cyclo-$(PR)_n$, where $\delta(^{31}P)$ depends on the average endocyclic P—P—P angle.[22] The cyclotriphosphanes (experimental[23] $\delta(^{31}P)$

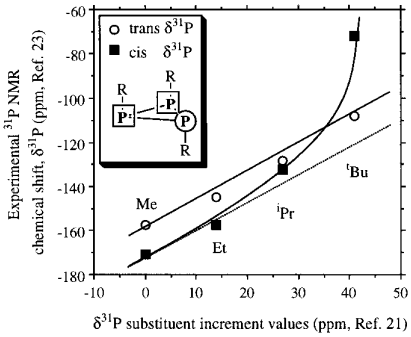

Figure 3. Experimental ^{31}P NMR chemical shifts, $\delta(^{31}P)$, of cyclotriphosphanes, cyclo-$(PR)_3$ (Ref. 23), versus the corresponding shift substituent increments derived from acyclic phosphanes (Ref. 21).

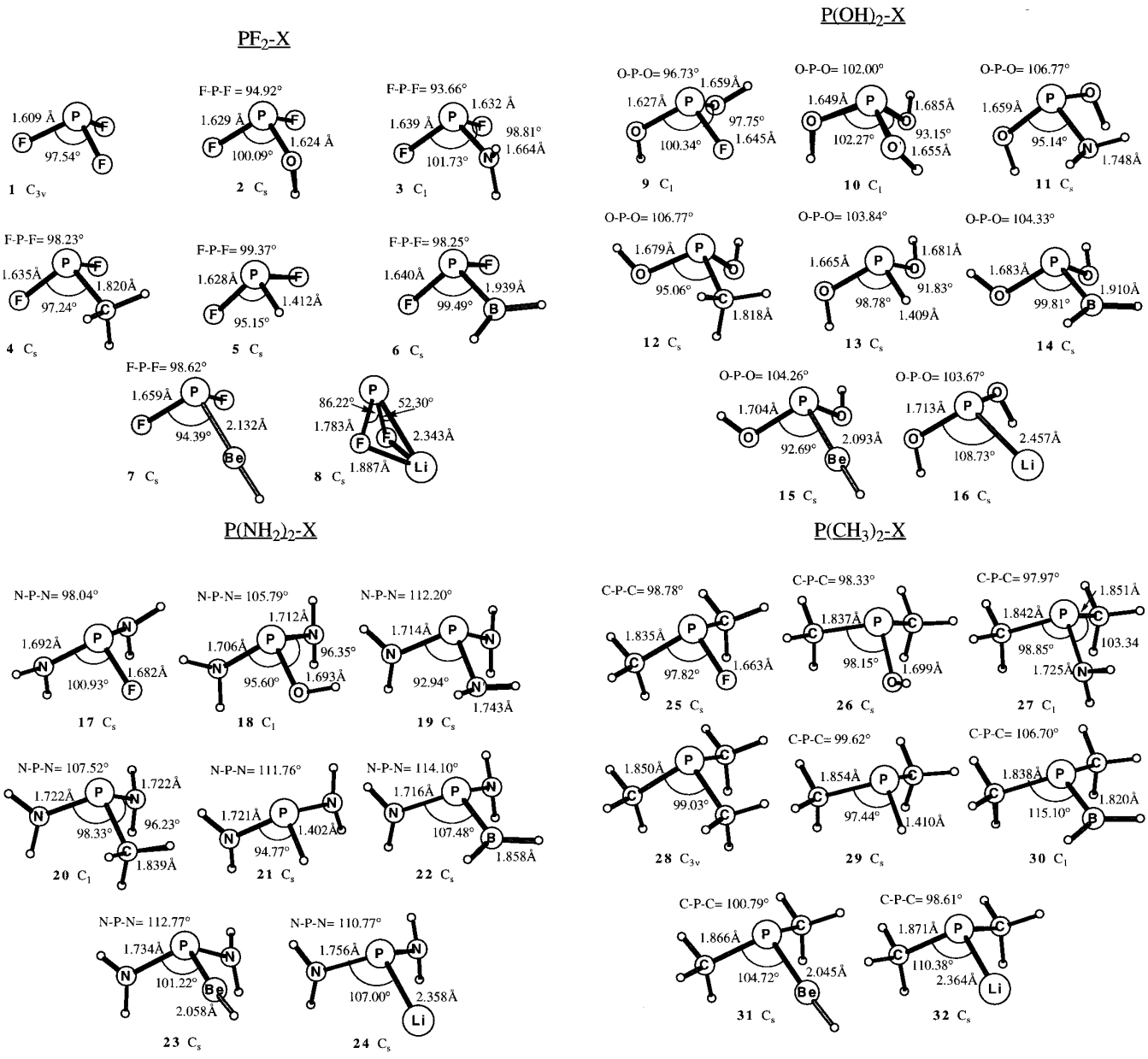

Figure 4. MP2(fc)/6–31 + G** geometries of PX_2Y molecules **1–64** (X, Y = H, Li, BeH, BH_2, CH_3, NH_2, OH and F).

for cyclo-$(PR)_3$ plotted against the $\Delta(\delta^{31}P)(R)$ increments[21,24] in Fig. 3) display especially instructive $\delta(^{31}P)$ values: while the shifts of the '*trans*' phosphorus is in good agreement with Maier's alkyl increments,[21,24] the two '*cis*'-substituted phosphoruses display marked deviations when bulky substituents (^{i}Pr, ^{t}Bu) are present. These are associated with the distinctly widened '*cis*' ^{t}Bu—P—P angle of 123° (known from the crystal structure).[23] The effect of widened H—P—H bond angles in PH_3 on $\delta(^{31}P)$ is not linear according to *ab initio* calculations.[25] The maximum of the $\delta(^{31}P)$–α(HPH) curve occurs around $\alpha(HPH) = 110°$ ($\delta(^{31}P) = -193$, C_{3v} symmetry), whereas the PH_3 minimum geometry ($\alpha(HPH) = 93.3°$) and the phosphorus inversion transition structure (planar tricoordinate phosphorus) have similar $\delta(^{31}P)$s upfield at −240 and −250 ppm, respectively. This stresses that bond angle–chemical shift regularities[22] depend 'on the fact that these correlations deal with only a limited structural variation.'[26] In representative sets of molecules, bond angle influences are often overshadowed by other factors.

'The most deshielded of "normal" phosphorus compounds is $PF_2(CH_3)$ at +245 ppm.'[27] This value is out-of-line with regard both to PF_3 ($\delta = 97$[28]) and to $PF(CH_3)_2$ ($\delta = 185$[29]). Differences in bond angles are not responsible [note the bond angle sums[30] of PF_3 (292.6°), $PF_2(CH_3)$ (292.7°), $PF(CH_3)_2$ (294.4°) and $P(CH_3)_3$ (297.1°) with $\delta(^{31}P) = -99$[2]]. The $\delta(^{31}P)$ estimates of $PF(CH_3)_2$ and $PF_2(CH_3)$ display the largest deviations (−207 and −217 ppm) in the set of molecules considered (Fig. 1). Is the PF fragment problematic? Not according to Fig. 1, where PF_3 and $PF_2(OMe)$ behave normally. Nevertheless, the largest

deviations in Fig. 1 are found for molecules with highly electronegative substituents, although none of these substituents is bulky.

We have chosen model compounds with small groups ('simple first-row substituents,' X, Y = H, Li, BeH, BH_2, CH_3, NH_2, OH and F, **1–64**) attached to σ^3,λ^3-phosphorus[31] because their geometrical effects should be negligible small. Unfortunately, experimental $\delta(^{31}P)$ data for most of the PX_2Y molecules with 'simple first-row substituents' (referred to as 'first-row sweep')[32] are not available (Table 2). However, *ab initio* NMR computations (IGLO,[11] GIAO[33]) can provide reasonably accurate data for such compounds (rmse of about 25 ppm, range over 850 ppm). The *ab initio*-derived data were analyzed to find relationships between the substitution on tricoordinate phosphorus and its NMR chemical shift by considering orbital interactions (based on NBO[34] population analysis), bond angles (based on RMP2(fc)/6–31 + G** optimized[35] geometries) and substituent electronegativities[20] (based on the Allred–Rochow[19] scale). Principle component analysis[36] is used to identify the most significant factors.[17] Molecules with three different 'simple first-row substituents', PXYZ, were then used to investigate whether the results for PX_2Y phosphanes can be generalized to the complete set[37b] of all 120 'simple' phosphanes.

COMPUTATIONAL METHODS

Using the Gaussian 94 program,[38] MP2(fc)/6–31 + G**[32] geometry optimizations were carried out for PX_2Y (**1–64**, Fig. 4) and PXYZ (**65–120**) phosphanes,[37] with 'simple first-row substituents' (X, Y = H,

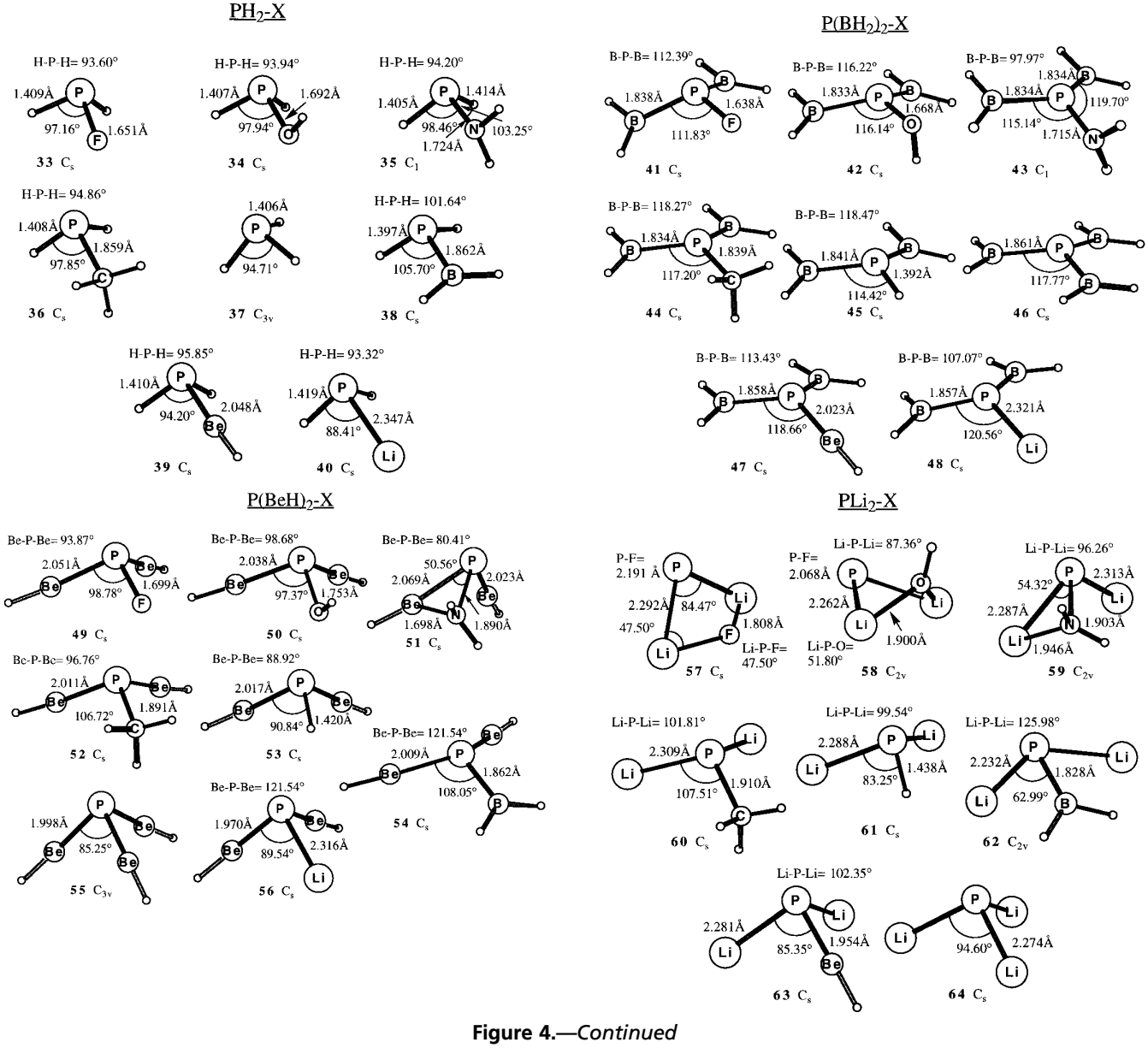

Figure 4.—*Continued*

Table 3. Calculated ^{31}P NMR chemical shifts, $\delta(^{31}P)$[a], substituent electronegativity sums, $\sum EN$[b], bond angle sums, $\sum \alpha$[c], electronic parameters [q(P)[d], sp^x and χ_p[e], E_{nhc}[f], ε_{HOMO} and ε_{LUMO}[g]], IGLO-computed chemical shifts, $\delta(^{31}P)_{IGLO}$[h], the $\delta(^{31}P)_{IGLO}$ contribution from the phosphorus lone pair, $-\Delta\sigma(^{31}P)(Lp(P))$[h] and ^{31}P shift estimates, $\delta(^{31}P)_{PCA}$[i], for PX_2Y phosphanes with X = H, Li, BeH, BH_2, CH_3, NH_2, OH and F (Fig. 4)

No.	Molecule	$\delta(^{31}P)$[a]	$\sum EN$[b]	$\sum \alpha$[c]	q(P)[d]	sp^x [e]	χ_p [e]	E_{nhc}[f]	ε_{HOMO}[g]	ε_{LUMO}[g]	$-\Delta\sigma(^{31}P)(Lp(P))$[h]	$\delta(^{31}P)_{IGLO}$[h]	$\delta(^{31}P)_{PCA}$[i]
1	PF_3	112.2	12.3	292.6	1.84	1.0	1.53	72.4	−0.48679	0.05988	226.2	95.7	233.2
2	$PF_2(OH)$	120.6	11.7	295.1	1.78	1.1	1.62	66.6	−0.46256	0.06504	225.6	103.6	193.2
3	$PF_2(NH_2)$	145.6	11.27	294.2	1.68	1.2	1.77	66.1	−0.43576	0.05561	233.5	129.7	182.4
4	$PF_2(CH_3)$	243.5	10.7	292.7	1.53	1.3	1.90	35.4	−0.41016	0.05533	266.8	224.7	146.3
5	PF_2H	211.2	10.4	289.7	1.40	1.3	1.98	38.1	−0.43182	0.05565	268.6	193.5	122.3
6	$PF_2(BH_2)$	295.7	10.3	297.2	1.22	1.4	2.19	46.8	−0.39313	0.00686	286.1	278.5	215.6
7	$PF_2(BeH)$	391.3	9.67	287.4	0.76	1.5	2.49	29.5	−0.37208	0.01710	325.8	363.3	141.9
9	$PF(OH)_2$	129.9	11.1	294.8	1.70	1.1	1.73	62.6	−0.42810	0.05525	225.0	115.5	174.1
10	$P(OH)_3$	118.5	10.5	297.4	1.64	1.2	1.81	55.8	−0.40348	0.05848	216.9	105.5	137.7
11	$P(OH)_2(NH_2)$	109.1	10.07	297.1	1.55	1.3	1.92	49.7	−0.37507	0.05713	209.6	98.7	113.9
12	$P(OH)_2(CH_3)$	157.9	9.5	293.5	1.33	1.5	2.15	36.6	−0.36484	0.05639	221.5	145.3	74.6
13	$P(OH)_2H$	130.8	9.2	294.4	1.23	1.5	2.21	57.8	−0.38658	0.06017	226.5	119.7	51.9
14	$P(OH)_2(BH_2)$	186.5	9.1	303.9	1.01	1.7	2.47	32.8	−0.35247	0.02690	227.1	176.4	121.8
15	$P(OH)_2(BeH)$	223.4	8.47	298.8	0.57	1.7	2.74	31.5	−0.33722	0.02409	250.4	207.9	79.8
16	$P(OH)_2Li$	388.6	7.97	321.1	0.44	1.7	2.85	28.4	−0.24179	0.02203	290.1	351.0	172.3
17	$PF(NH_2)_2$	126.1	10.24	299.9	1.51	1.4	1.99	53.5	−0.39786	0.06493	212.6	109.8	115.7
18	$P(OH)(NH_2)_2$	103.6	9.64	297.7	1.43	1.5	2.09	43.9	−0.36407	0.06427	205.2	93.7	77.1
19	$P(NH_2)_3$	66.5	9.21	298.1	1.33	1.6	2.20	45.1	−0.33550	0.06349	187.5	59.3	53.6
20	$P(NH_2)_2(CH_3)$	23.9	8.64	302.1	1.19	1.7	2.38	30.6	−0.34669	0.06061	162.9	15.7	32.3
21	$P(NH_2)_2H$	6.0	8.34	301.3	1.02	1.7	2.49	35.4	−0.36302	0.05711	166.5	0.0	19.1
22	$P(NH_2)_2(BH_2)$	50.8	8.24	329.0	0.89	2.2	2.79	36.0	−0.32982	0.03377	143.9	45.4	105.7
23	$P(NH_2)_2(BeH)$	15.8	7.61	315.2	0.34	2.0	3.07	30.3	−0.32030	0.02823	159.3	11.6	52.16
24	$P(NH_2)_2Li$	89.1	7.11	324.8	0.18	2.0	3.18	28.1	−0.23293	−0.01130	185.7	81.1	109.4
25	$PF(CH_3)_2$	173.1	9.1	294.4	1.19	1.6	2.30	12.3	−0.36553	0.05797	222.8	156.0	49.8
26	$P(OH)(CH_3)_2$	87.4	8.5	294.6	1.08	1.7	2.43	13.5	−0.34635	0.06132	186.0	75.4	8.7
27	$P(NH_2)(CH_3)_2$	−10.6	8.07	300.2	1.01	1.8	2.55	13.3	−0.33872	0.05774	146.2	−19.4	−0.1
28	$P(CH_3)_3$	−80.9	7.5	297.1	0.81	1.9	2.75	0.0	−0.32987	0.05598	117.1	−92.0	−36.6
29	$P(CH_3)_2H$	−110.6	7.2	294.5	0.62	2.0	2.89	0.0	−0.34323	0.05949	115.4	−117.4	−65.4
30	$P(CH_3)_2(BH_2)$	−29.9	7.1	336.9	0.55	2.5	3.18	0.0	−0.31169	0.04511	144.6	−32.4	32.9
31	$P(CH_3)_2(BeH)$	−148.1	6.47	310.1	−0.08	2.3	3.51	0.0	−0.30835	0.03371	90.7	−152.0	−34.6
32	$P(CH_3)_2Li$	−119.3	5.97	319.4	−0.18	2.3	3.58	0.0	−0.22461	−0.01230	114.0	−112.4	33.3
33	PFH_2	94.7	8.5	287.9	0.84	1.6	2.56	0.0	−0.40504	0.05173	209.2	82.2	12.9
34	$P(OH)H_2$	18.6	7.9	289.8	0.72	1.8	2.71	13.5	−0.37954	0.05794	175.0	10.5	−29.9
35	$P(NH_2)H_2$	−84.0	7.47	295.9	0.63	1.9	2.85	13.4	−0.36982	0.05790	134.1	−84.2	−44.0
36	$P(CH_3)H_2$	−166.3	6.9	290.6	0.39	2.0	3.07	0.0	−0.36055	0.05728	99.5	−168.9	−86.7
37	PH_3	−240.0	6.6	284.1	0.15	2.1	3.27	0.0	−0.38412	0.06314	73.4	−240.0	−126.9
38	$P(BH_2)H_2$	−152.9	6.5	313.0	0.05	2.4	3.49	0.0	−0.35949	0.04697	63.2	−147.1	−50.5
39	$P(BeH)H_2$	−292.3	5.87	284.3	−0.55	2.3	3.87	0.0	−0.35809	0.03059	39.1	−181.9	−113.0
40	PH_2Li	−341.4	5.37	270.1	−0.70	2.4	4.00	0.0	−0.26614	−0.01387	35.8	−302.0	−91.7
41	$PF(BH_2)_2$	269.1	8.3	336.0	0.68	2.3	2.98	11.9	−0.36458	0.03328	171.4	264.6	123.2
42	$P(OH)(BH_2)_2$	186.1	7.7	348.5	0.63	2.5	3.11	14.7	−0.34559	0.03591	134.9	188.1	106.3
43	$P(NH_2)(BH_2)_2$	102.1	7.27	353.5	0.48	2.8	3.30	13.6	−0.33552	0.04400	95.5	106.4	76.0
44	$P(CH_3)(BH_2)_2$	30.6	6.7	352.7	0.26	2.9	3.51	0.0	−0.32914	0.04068	61.2	35.0	46.5
45	$P(BH_2)_2H$	−21.5	6.4	347.3	0.01	2.9	3.69	0.0	−0.34892	0.03822	53.4	−15.7	22.8
46	$P(BH_2)_3$	45.5	6.3	353.3	−0.12	3.0	3.83	0.0	−0.35302	0.03755	49.0	51.4	29.3
47	$P(BH_2)(BeH)$	−35.0	5.67	350.7	−0.69	2.9	4.24	0.0	−0.34325	0.03380	35.1	−26.4	−6.4
48	$P(BH_2)_2Li$	−17.2	5.17	348.3	−0.73	2.8	4.22	0.0	−0.28536	−0.01885	36.0	4.6	51.3
49	$PF(BeH)_2$	298.5	7.04	291.4	−0.48	2.1	3.67	3.5	−0.36112	0.00304	204.9	275.4	17.7
50	$P(OH)(BeH)_2$	138.1	6.44	293.4	−0.63	2.2	3.84	1.9	−0.34326	0.01542	155.3	126.4	−35.7
52	$P(CH_3)(BeH)_2$	−198.2	5.44	310.2	−1.02	2.6	4.31	0.0	−0.32613	0.02197	36.8	−191.8	−75.1
53	$P(BeH)_2H$	−278.7	5.14	270.6	−1.21	2.5	4.42	0.0	−0.36541	0.02938	9.6	−265.3	−179.9
54	$P(BH_2)(BeH)_2$	−145.1	5.04	337.6	−1.32	2.9	4.68	0.0	−0.33904	0.02523	11.0	−133.4	−53.3
55	$P(BeH)_3$	−186.8	4.41	255.7	−1.79	2.7	4.92	0.0	−0.38458	0.02916	−13.7	−177.2	−250.8
56	$P(BeH)_2Li$	−172.8	3.91	261.3	−1.99	2.8	5.10	0.0	−0.30331	−0.01691	13.0	−154.8	−189.5
60	$P(CH_3)Li_2$	−168.3	4.44	316.8	−1.25	2.5	4.47	0.0	−0.19846	−0.00431	…	…	−76.3
61	PLi_2H	−351.0	4.14	266.0	−1.55	2.6	4.72	0.0	−0.22075	−0.00531	…	…	−187.3
63	$P(BeH)Li_2$	−188.2	3.41	273.1	−2.20	2.8	5.30	0.0	−0.24362	−0.00730	…	…	−214.0
64	PLi_3	−202.7	2.91	283.8	−2.40	2.8	5.47	0.0	−0.19862	−0.00185	…	…	−233.2

[a] GIAO/6–311 + G**//MP2(fc)/6–31 + G**.

[b] The substituent electronegativity (e.g. EN(X) for X) is approximated by the Allred–Rochow electronegativity[19,20] of the atom attached to phosphorus.

[c] Bond angle sums at phosphorus.

[d] Atomic charge of phosphorus from NAO population analysis (Ref. 34).

[e] Occupancy of the valence s-, p- and d-AOs (χ_s, χ_p, χ_d) on phosphorus from NAO population analysis:[34] valence 'hybridization' characterized by sp^x, which is the χ_p/χ_s ratio; χ_d values are all below 0.07.

[f] Energy from NBO[34] population analysis describing the extent of negative hyperconjugation (nhc); see Computational Methods.

[g] Energy of the highest occupied and lowest unoccupied MO in hartrees.

[h] IGLO/BII[11]//MP2(fc)/6–31 + G**; $-\Delta\sigma(^{31}P)(Lp(P))$ is the contribution to the $\delta(^{31}P)_{IGLO}$ value from the localized lone pair orbital (isotropic magnetic shielding contribution of the phosphorus lone pair multiplied by minus one).

[i] Estimates from eqn (2), derived from principle component analysis. $\delta(^{31}P)_{PCA} = -940 + 59.4 \sum EN + 1.87 \sum \alpha - 1746\varepsilon_{LUMO}$.

Li, BeH, BH_2, CH_3, NH_2, OH, F). Analytical second derivatives[39] established the nature of stationary points at the same level. The '0 K' or 'frozen' geometries do not necessarily describe the real chemical shift average correctly but provide systematically defined structures.[40,41] NMR chemical shifts (Table 3) were calculated with GIAO[42,43]/6–311 + G** on the lowest energy MP2 minima (structures **8**, **51**, **57–59** and **62** omitted). Computations using three sets of *d* functions instead of only one as in the 6–311 + G** basis set changes the computed absolute magnetic shieldings.[25,44] Nevertheless, these changes are for the most part compensated[45] in the NMR chemical shifts, $\delta(^{31}P)$, presented in Table 3.

The physical basis of NMR, the Zeeman effect, is modeled in *ab initio* computations. For the 'bare nucleus'[46] (no electrons around the nucleus), the flip of the nuclear magnetic spin, μ_k, in an external magnetic field, B, is associated with the energy difference ΔE_A (Fig. 5, Eqn (A);[47] if ΔE_A was not quantized no characteristic transition could be observed). For atoms the energy of the μ_k flipping (the NMR shielding constant) is simply a function of the spherical charge density [Fig. 5, Eqn (B)]. 'This is known as Lamb's formula; an equivalent expression may be derived quantum mechanically.'[49]

Lamb's formula includes a simple relationship between the electron density around a nucleus and its NMR chemical shift, $\delta(^{31}P)$, which tempts one to apply 'charge-shift' rules to non-atomic systems. Furthermore, the 'classical' physical approach[50] simplifies the interaction of the electrons in a molecule with the external field to a local 'effective field' ($B_{loc} = B_0(1 + \sigma)$; e.g. σ_k at the position of μ_k). In the electromagnetic (em) picture $\Delta E_{em}(\mu_k$ flip) is described by $\Delta\mu_k B_{loc}$ (Fig. 5, Eqn (B′)). For more complex systems than atoms (e.g. H_2), corrections of the Lamb equation are required because the several 'nuclei prevent a simple circular diamagnetic circuit of the electrons' about a nucleus in a molecule.[51] In contrast to the electromagnetic picture, the quantum mechanical (QM) approach[52] describes the influence of the magnetic field (external and from μ_k) on the energy of the electrons (Fig. 5, Eqn (C): $\Delta E_{QM}(\mu_k$ flip) is the change of electronic energy of the molecule, E). In the QM treatment, the μ flip of a nucleus changes of the molecular energy, ΔE_{QM} (Fig. 5, Eqn (C); this interaction of μ_k with the nearby electrons has a similar energetic effect in comparable 'chemical surroundings,' causing similar NMR 'chemical shifts'). 'The simple classical [electrodynamic] model fails for molecules, as the charge distribution here is not usually spherically symmetric. Attempts were nevertheless made to apply it'[7] because it is much easier in practice than the QM description. Therefore, ignorance of this limitation of classical physics to explain the chemical shift, which is a quantum mechanical phenomenon, 'by assuming that the magnetic field B_0 induces an electron current in the electron shell'[7] with a magnetic field opposing B_0 [Fig. 5, Eqn (B′)][53] is probably the reason for some misunderstandings between theoretical and pragmatic chemists on the 'physical basis' of NMR effects.

The *ab initio* equations do not reveal any simple relationship between the electron density around a nucleus and its chemical shift. *Ab initio* $\delta_{calc}(^{31}P)$ data can be analyzed along with experimental values in empirical approaches to seek ^{31}P NMR chemical shift relationships. Other approaches separate effects on $\delta_{calc}(^{31}P)$ into dia-, para- and other magnetic contributions,[54] but we apply statistical analysis (see below) to search for 'general' (for the complete set) or 'local' (for subsets) relationships of geometric (e.g. bond angle sum) or electronic parameters (e.g. charge distribution and

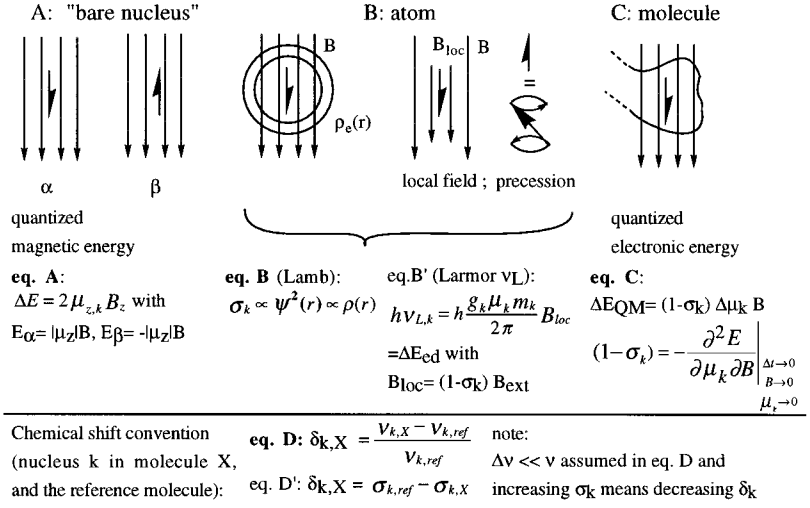

Figure 5. Schematic description and equations of the nuclear magnetic shielding in case of (A) a 'bare nucleus,' (B) an atom and (C) a molecule. Notation: B is an external magnetic field (B_z its component in the z-direction); μ_k is the magnetic moment of the nucleus k; σ_k is the magnetic shielding constant, a tensor, of nucleus k; E is the energy of the system; h is Planck's constant. Most other constants are omitted for simplicity. The indices in Eqn (C) express that an infinitely fast flipping ($\Delta t \to 0$) and infinitely small magnetic fields ($B \to 0$, $\mu_k \to 0$) are assumed (otherwise a time-dependent Schrödinger equation must be solved and effects, e.g. magnetic susceptibility, would have to be taken into account).

conjugation) with $\delta_{calc}(^{31}P)$ of tricoordinate phosphorus. Statistical errors are characterized by the rmse and by the square of the correlation coefficient, cc.[36] Only correlation lines with cc values larger than 0.9 characterize *correlations*. We have also employed principle component analysis:[36] the best descriptor[17] (that leads to the largest cc) is used to set up an equation for $\delta(^{31}P)$. Other descriptors[17] are included in like manner to improve the performance. This refinement is continued until no independent descriptor has a cc above 0.1. Relationships of $\delta(^{31}P)$ with 'local' character are discussed in the sections about group A, B and C subsets of PX_2Y molecules.

The substituent electronegativity, e.g. *EN*(X) and *EN*(Y), is approximated by the Allred–Rochow[19] electronegativity of the element E in the EH_n group. The bond angle sum, $\sum \alpha$, is defined by the three angles involving tricoordinate phosphorus, e.g. $\sum \alpha = \alpha(XPY) + \alpha(YPX') + \alpha(X'PX)$. The atomic charge, q, and the phosphorus hybridization, sp^x, is derived by natural orbital localization in the natural population analysis (RHF/6–311 + G**//MP2(fc)/6–31 + G*).[34,55] Reed and Schleyer[56] have shown that negative hyperconjugation is especially important for tricoordinate derivatives because phosphorus has an intermediate electronegativity. The extent of *negative hyperconjugation*, E_{nhc} (Table 3), is defined by the energy in the second-order NBO perturbation theory analysis of the fock matrix which can be associated with orbital interactions between a lone pair on a substituent, X, and a P—Y antibonding orbital [e.g. $Lp(X) \rightarrow \sigma^*(P—Y)$]. Generally, 'according to the NBO analysis,[56] hyperconjugation represents the charge delocalization which is necessary to describe electron distributions adequately and which is not accounted for when a molecule is build up from strictly localized orbitals (NBOs).'[57]

RESULTS AND DISCUSSION

The computed ^{31}P NMR chemical shifts, $\delta(^{31}P)$ (Table 3) for the complete PX_2Y set (with X, Y = H, Li, ..., F), are used to explore both general and local relationships with the substituent electronegativity sum, $\sum EN$, the bond angle sum, $\sum \alpha$, and other descriptors. Subsets of the PX_2Y molecules with X = Li, BeH (group A), X = BH_2, H, CH_3 (group B) and X = NH_2, OH, F (group C) are analyzed separately, seeking 'local' relationships. The large influence of negative hyperconjugation[56] (see computational methods) in the PF_2Y subset is discussed in group C. Finally, the apparent $\delta(^{31}P)$–$\sum EN$ relationship in the experimentally important PXYZ molecules (Table 3 and supplementary information) is demonstrated.

NMR chemical shift and substituent electronegativity sum

Whereas *ab initio*-optimized geometries, molecular orbital energies and electron distribution (population analysis) must be computed, the substituent electronegativity sum, $\sum EN$, is obtained by simple addition. The $\sum EN$–$\delta(^{31}P)$ plot (Fig. 6, $\sum EN$, ranging from 2.9 to 12.3) shows considerable scatter with a lower limit [$\delta(^{31}P) > -2024 + 391 \sum EN - 18 (\sum EN)^2$] mainly defined by the subset with 'common' substituents (X, Y = H, CH_3, NH_2, OH and F; filled circles in Fig. 6). However, no correlation is present for the complete set of PX_2Y with X, Y = H and Li to F. Nevertheless, local correlations can be found in some subsets (see Fig. 2 and the discussions of the groups A, B and C).

^{31}P NMR chemical shift and bond angle sum

In general, the $\delta(^{31}P)$ values of our set of PX_2Y molecules do not correlate with $\sum \alpha$ (Fig. 7). Not even the geometries of one molecule with different $\sum \alpha$ values give linear $\sum \alpha - \delta(^{31}P)$ relationships (see the lines through the filled symbols in Fig. 7) for computed $\delta(^{31}P)$ for C_{3v} symmetric PZ_3 molecules with various Z—P—Z angles (data can be found in the supplementary materia).

Similar previous studies[25,58] analyzed the non-linear relationship of $\delta(^{31}P)$ of PH_3 with various bond angles (both rigid and optimized P—H bond lengths were used). The difference between the $\delta(^{31}P)$ for deformed structures with fixed or with optimized P—Z bond lengths is small (e.g. 5 ppm for PMe_3 with a fixed C—P—C angle of 105°). The $\delta(^{31}P)$–$\sum \alpha$ slopes [tangents of the $\delta(^{31}P)$–$\sum \alpha$ curves depicted in Fig. 7] of PH_3 [**37**, $(\sum \alpha)_{min} = 284.13°$], PMe_3 [**28**, $(\sum \alpha)_{min} = 297.09°$] and PF_3 [**1**, $(\sum \alpha)_{min} = 292.62°$] at their minimum geometry are 1.7, 1.6 and only 0.3 ppm per degree ($\sum \alpha$). Nevertheless, changing all three phosphorus bond angles is likely to have a different effect on $\delta(^{31}P)$ than changing only one or two angles (e.g. one endocyclic P—P—P angle with a $\delta(^{31}P)$–α slope[22] of 3 ppm per degree). The largest changes of $\delta(^{31}P)$ with $\sum \alpha$ are less than 65 ppm (deformed PMe_3) and much

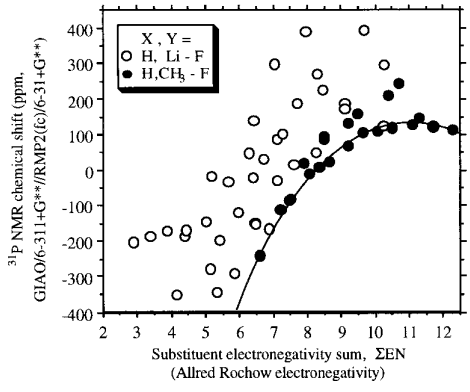

Figure 6. Calculated ^{31}P NMR chemical shifts [GIAO/6–311 + G**//RMP2(fc)/6–31 + G**] versus the substituent electronegativity sum, $\sum EN = EN(Y) + 2EN(X)$, for PX_2Y (X, Y = H, Li, F and the subset X, Y = H, CH_3, F. Although the variation in $\delta(^{31}P)$ is over 400 ppm for a given $\sum EN$, the lower limit [$\delta(^{31}P) > -2024 + 391 \sum EN - 18 (\sum EN)^2$] is apparent.

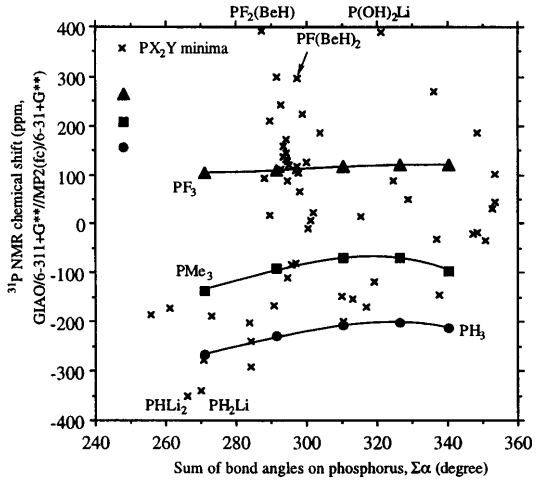

Figure 7. Calculated [GIAO/6–311 + G**//MP2(fc)/6–31 + G**] ^{31}P NMR chemical shifts versus the phosphorus bond angle sum [MP2(fc)/6–31 + G**] of PX_2Y with X, Y = H, Li, BeH, BH_2, CH_3, NH_2, OH, F. The figure shows the lack of a significant $\sum \alpha$–$\delta(^{31}P)$ relationship. The values for PF_3, $P(CH_3)_3$ and PH_3 with only the bond angles varied are added as support.

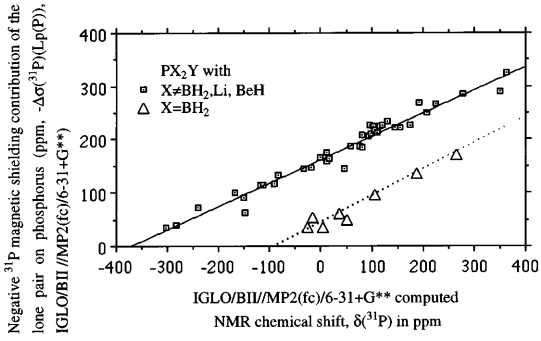

Figure 8. IGLO/BII//MP2(fc)/6–31 + G** computed negative ^{31}P magnetic shielding contribution of the lone pair on phosphorus, $-\Delta\sigma(^{31}P)$[Lp(P)], versus (total) ^{31}P NMR shift, $\delta(^{31}P)$, for $P(BH_2)_2Y$ (dotted line: slope 0.41; cc: 0.959) and for PX_2Y with $X \neq BH_2$, Li, BeH (solid line: slope 0.45; cc = 0.958).

smaller than the total range of the ^{31}P shifts considered (about 800 ppm, Fig. 7). Therefore, other influences on $\delta(^{31}P)$ should be more important in the PX_2Y phosphanes, **1**–**64**, than the bond angle sum. Nevertheless, $\delta(^{31}P)$ may be sensitive to the bond angles in systems with similar phosphorus environments, e.g. the cyclo-$(PR)_3$ in Fig. 3; see Ref. 23).

$\sum$ *EN* and molecular orbitals (MO)

The PX_2Y HOMOs can be characterized as non-bonding electron pairs on phosphorus, Lp(P). Even though the HOMO energy does not correlate with $\delta(^{31}P)$, details of the contributions of the electrons of the Lp(P) to the total magnetic shielding are interesting. Bond increments [e.g. for $\delta(^{31}P)$] require constant bond orbital contributions. How can the contribution of the Lp(P) to $\delta(^{31}P)$ be quantified?

The distribution of electrons in a molecule can be described by various localized representations.[10,56,59] Foster–Boys localized[10] MO, LMO representations comprise bond orbitals and non-bonding orbitals [e.g. Lp(P)]. The contribution of an LMO [e.g. of the Lp(P) LMO] to the total magnetic shielding[45] [e.g. of phosphorus, $\sigma(^{31}P)$] can be calculated by the IGLO[11] or the LORG[60] program. The negative Lp(P) contribution to $\sigma(^{31}P)$, $-\Delta\sigma(^{31}P)$(Lp(P)), is plotted against the (total) chemical shift[45] in Fig. 8 (values in Table 3). The $-\Delta\sigma(^{31}P)$(Lp(P)) are all positive [deshielding; except $P(BeH)_3$ with −13.7 ppm, not depicted in Fig. 8], and obviously not constant (ranging over 300 ppm; compare $PH_{3-n}F_n$[11] in the Introduction). Therefore, it is not reasonable to set up, respectively, a $\sigma(^{31}P)$ or $\delta(^{31}P)$ bond increment for Lp(P). Interestingly, the slope of the $-\Delta\sigma(^{31}P)$(Lp(P))–$\delta(^{31}P)$ regression line is approximately 0.4 (solid line in Fig. 8). This means that more than a third of the change in $\sigma(^{31}P)$ is due to the Lp(P) contribution.

The $-\Delta\sigma(^{31}P)$(Lp(P))–$\delta(^{31}P)$ regression line (dotted line drawn through the triangles in Fig. 8) for $P(BH_2)_2Y$ molecules shows a 100 ppm offset with respect to the corresponding line (solid in Fig. 8) for most other PX_2Y (squares, solid line in Fig. 8, PX_2Y with X = Li, BeH and BH_2 neglected). This systematic deviation can be associated with the special character of the B—P—B bonding (allyl cation character; see also discussion of group B subsets).

Statistical relationship between $\delta(^{31}P)$ and other parameters

Besides $\sum$ *EN* and $\sum \alpha$, we considered various electronic factors[17] derived from the *ab initio* calculations (see Table 4; the descriptors are discussed in detail below): the atomic charges of phosphorus, q(P), the occupancy of p- and d-type atomic orbitals, χ_p and χ_d, together with the phosphorus valence hybridization, sp^x, the HOMO and the LUMO energies, ε_{HOMO} and ε_{LUMO}, and the extent of negative hyperconjugation, E_{nhc}. The table of correlation coefficients (Table 4) shows that $\delta(^{31}P)$ is best related with $\sum$ *EN* (cc = 0.527). Several electronic descriptors are poorly related to $\delta(^{31}P)$ but correlate better with $\sum$ *EN*: q(P), χ_p (hybridization, sp^x, E_{nhc}, χ_d and ε_{HOMO} have cc between 0.9 and 0.5). In contrast, $\sum \alpha$ and ε_{LUMO} do not correlate with $\sum$ *EN*. Thus, principle component analysis (PCA)[36] leads to a description given by

$$\delta(^{31}P)_{PCA} = -940 + 59.4 \sum EN + 1.87 \sum \alpha - 1746\varepsilon_{LUMO} \quad (2)$$

The $\delta(^{31}P)$–$\sum$ *EN* relationship [$\delta(^{31}P) = -390 + 59 \sum EN$] itself reproduces our $\delta(^{31}P)$ values with an rmse of 122 ppm.[61] Including a bond angle sums term reduces the rmse to 113 ppm. For comparison, the shift estimates, $\delta(^{31}P)_{PCA}$, derived with Eqn (2) give an rmse of 103 ppm.

Table 4. Correlation coefficients (c) and their squares (cc, in parentheses) between the calculated[a] NMR chemical shift of phosphorus, $\delta(^{31}P)$[a], the substituent electronegativity sum[b], the bond angle sum[c], electronic parameters (q(P)[d], sp^x and χ_p[e], E_{nhc}[f], ε_{HOMO} and ε_{LUMO}[g]), and the $\delta(^{31}P)_{IGLO}$ contribution[h] from the phosphorus lone pair in PX_2Y phosphanes with X = H, Li, BeH, BH_2, CH_3, NH_2, OH and F

	$\delta(^{31}P)$[a]	ΣEN[b]	q(P)[d]	χ_p[e]	E_{nhc}[f]	sp^x[e]	ε_{HOMO}[g]	$\sum\alpha$[c]	ε_{LUMO}[g]	$-\Delta\sigma(^{31}P)$(Lp(P))[h]
$\delta(^{31}P)$[a]	...	(0.527)	(0.432)	(0.445)	(0.347)	(0.333)	(0.171)	(0.058)	(0.036)	(0.743)
$\sum EN$[b]	0.726	...	(0.910)	(0.947)	(0.743)	(0.810)	(0.553)	(0.000)	(0.394)	(0.729)
q(P)[d]	0.657	0.954	...	(0.978)	(0.565)	(0.692)	(0.437)	(0.011)	(0.503)	(0.617)
χ_p[e]	−0.667	−0.973	−0.989	...	(0.635)	(0.810)	(0.452)	(0.089)	(0.461)	(0.699)
E_{nhc}[f]	0.589	−0.862	0.752	−0.797	...	(0.688)	(0.321)	(0.015)	(0.175)	(0.552)
sp^x[e]	−0.577	−0.900	−0.832	0.900	−0.829	...	(0.369)	(0.136)	(0.273)	(0.746)
ε_{HOMO}[g]	−0.239	−0.744	−0.661	0.672	−0.567	0.607	...	(0.020)	(0.550)	(0.192)
$\sum\alpha$[c]	0.242	−0.020	−0.105	−0.299	−0.122	0.369	0.141	...	(0.001)	(0.009)
ε_{LUMO}[g]	0.189	0.628	0.709	−0.679	0.418	−0.522	−0.742	−0.032	...	(0.096)
ΔLp(P)[h]	−0.862	−0.854	−0.786	0.836	−0.743	0.864	0.438	0.095	−0.309	...

[a] GIAO/6–311 + G**//MP2(fc)/6–31 + G**.
[b] The substituent electronegativity (e.g. EN(X) for X) is approximated by the Allred–Rochow electronegativity[19,20] of the atom attached to phosphorus.
[c] Bond angle sums at phosphorus.
[d] Atomic charge of phosphorus from NAO population analysis (Ref. 34).
[e] Occupancy of the valence s-, p- and d-AOs (χ_s, χ_p, χ_d) on phosphorus from NAO population analysis:[34] valence 'hybridization' characterized by sp^x, which is the χ_p/χ_s ratio; χ_d values are too small (between 0.07 and zero) to give significant correlation coefficients.
[f] Energy from NBO[34] population analysis describing the extent of negative hyperconjugation (nhc); see text (Computational Methods).
[g] Energy of the highest occupied and lowest unoccupied MO in hartrees.
[h] Isotropic magnetic shielding contribution of the phosphorus lone pair computed at IGLO/BII[11]//MP2(fc)/6–31 + G** multiplied by minus one.

Figure 9 plots the estimated [Eqn (2)] compared with the *ab initio*-computed ^{31}P NMR shifts. Those molecules in Fig. 9 which display deviations between $\delta(^{31}P)_{PCA}$ and $\delta(^{31}P)$ larger than the rmse value (outside the area between the dotted lines) have either one or two Li or BeH substituents (e.g. PH_2Li, **40**, or $PHLi_2$, **61**; estimates deviate downfield) or a combination of these with electronegative substituents (deviations upfield; PF_2(BeH), **7**; and P(OH)$_2$Li, **16**). $\delta(^{31}P)_{PCA}$ deviations of the last group can be attributed to the neglect of the negative hyperconjugation effects on $\delta(^{31}P)$ (see discussion of group C subsets below). Generally, the statistically derived estimates do not work well (rmse > 100 ppm) in reproducing the $\delta(^{31}P)$ of PX_2Y phosphanes.

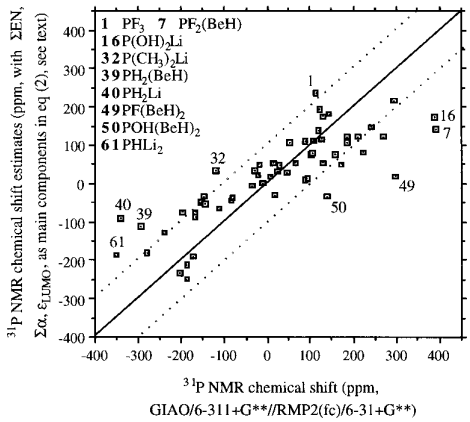

Figure 9. ^{31}P NMR chemical shift estimates ($\delta(^{31}P)_{PCA} = -940 + 59.4\sum EN + 1.87\sum\alpha - 1746\varepsilon_{LUMO}$; see text, Eqn (2) from main component analysis) versus calculated ^{31}P NMR chemical shifts (GIAO/6–311 + G**//RMP2(fc)/6–31 + G**) for PX_2Y (X, Y = 'first-row sweep,'[32] numbering as in Fig. 5 and Tables 3 and 4). Dotted lines in distance of the rmse (103 ppm) from the line of ideal agreement.

PX_2Y subsets with 'local' $\delta(^{31}P)$ relationships

Since no satisfactory, general relationship for $\delta(^{31}P)$ of PX_2Y (X, Y = H, Li, ..., F; Fig. 6) was found, we searched subsets A, B and C (parts of Fig. 6 in Figs 11–13) for 'local' relationships. While bridged structures (**8**, **51**, **57–59** and **62**) are left out in the search for such $\delta(^{31}P)$ substituent effect relationships because of their exceptional character, their geometries are interesting and are discussed first below.

PLi_2Y and P(BeH)$_2$Y (group A)

Minima with non-cyclic structure are found only for four of the eight PLi_2Ys considered. The PLi_2F, **57**, and PLi_2OH, **58**, minima (Fig. 5) might be described as double Li bridged PX dianions. The double Li bridging of the C_2 dianion in C_2Li_2[62] results in a significantly lengthened CC bond (1.28 Å compared with 1.20 Å in H—CC—H, MP2(fc)/6–31 + G**). Likewise, the P—F and P—OH distances (2.191 and 2.068 Å, respectively) are much larger than their 'normal' bond lengths (e.g. 1.651 Å in H_2P—F, **33**, and 1.692 Å in H_2P—OH, **34**). The four-membered P—Li—Y—Li rings in **57** (Y = F) and **58** (Y = OH) are puckered, as is the N—Li—O—Li fragment of the HC(=O)NLi_2'[62] molecule. The $PLi_2(NH_2)$ minimum, **59**, is characterized by one lithium bridging the P—N bond. The $PLi_2(BH_2)$ min-

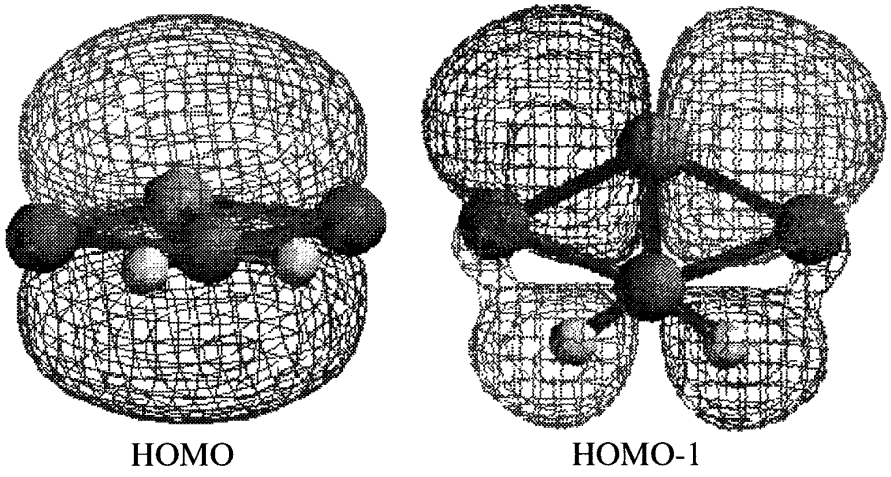

Figure 10. HOMO and HOMO-1 of PLi_2BH_2, **62** (RHF/6–31 + G**//MP2(fc)/6–31 + G**).

imum, **62**, is unusual since all atoms are in one plane and the Li—P—B bond angles are only 63°. This rhomboid structure, with short P—Li bonds compared with those in **60**, **61**, **63** and **64**, may be described as two Li cations coordinating on the side of an H_2B—P dianion π system (according to NBO population analysis; note that in $[B_2H_4]^{2-}(Li^+)^2$ the lithiums are also in-plane with all other atoms due to 'interaction between the in-plane π_{BH_2} orbitals and the unsymmetric combination of the lithium 2s atomic orbitals;'[63] see also HOMO-1 in Fig. 10). The HOMO of **62** (Fig. 10) shows a B—P π orbital deformed towards the Li cations. The preference of the lithiums for the position in the BH_2 plane is probably due to a Li–H interactions (HOMO-1, Fig. 10, B—H is polarized, partial negative charge on hydrogen attracts Li^+). In the $P(BeH)_2Y$ set only the minimum with $Y = NH_2$ has a bridged structure like that of $PLi_2(NH_2)$, **59**.

The $\delta(^{31}P)$ values for the non-cyclic molecules of group A are plotted against $\sum EN$ in Fig. 11 (open symbols) together with the chemical shift of the lowest energy transition structure of $P(BeH)_2NH_2$ (Fig. 11, crossed symbol). Whereas the four PLi_2Y points do not display an obvious order, the $P(BeH)_2Y$ subset can be divided in two clusters. In $P(BeH)_2Y$ with Y = Li, BeH, BH_2 and CH_3 the $\delta(^{31}P)$ is approximately constant (no dependence on $\sum EN$). In contrast, a large slope (300 ppm au^{-1}) is found for $P(BeH)_2Y$ with Y = F, OH, NH_2 (TS of X_2P–NH_2 rotation with Lp(N) and Lp(P) *anti*), CH_3 and H.

$P(BH_2)_2Y$, PH_2Y and $P(CH_3)_2Y$ (group B)

These sets show the most regular behavior compared with the other PX_2Y sets discussed, although $P(BH_2)_2Y$ is a special case. The cc values are 0.955 (X = H), 0.853 ($X = BH_2$) and 0.831 ($X = CH_3$) for the $\delta(^{31}P)$–$\sum EN$ relationship with similar slopes of 141 (X = H) and 98 ($X = BH_2$, CH_3) ppm per electronegativity 'unit' (Fig. 12). The downfield shift (reduced magnetic shielding) of $PX_2(BH_2)$ with respect to PX_2H and of $P(BH_2)_2Y$ compared with $P(CH_3)Y$ is due to the conjugation of the Lp(P) with an empty p-AO of the BH_2 substituent. Calculations of the transition structure, TS, of rotation

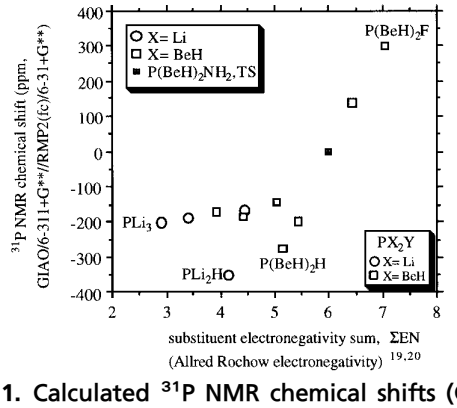

Figure 11. Calculated ^{31}P NMR chemical shifts (GIAO/6–311 + G**//RMP2(fc)/6–31 + G**) versus the substituent electronegativity sum, $\sum EN$ (Allred–Rochow electronegativity), for a subset (X = Li, BeH and 'first-row sweep'[32] of Y) of the PX_2Y in Fig. 6 ('first-row sweep'[32] of X and Y) augmented by the value for the lowest energy transition structure of $P(BeH)_2NH_2$.

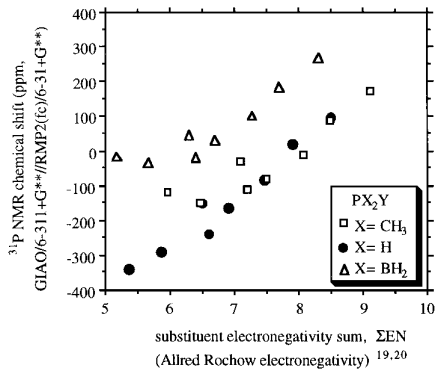

Figure 12. Calculated ^{31}P NMR chemical shifts (GIAO/6–311 + G**//RMP2(fc)/6–31 + G**) versus the substituent electronegativity sum, $\sum EN$ (Allred–Rochow electronegativity), for a subset (X = H, BH_2, CH_3 and 'first-row sweep'[32] of Y) of the PX_2Y in Fig. 6 ('first-row sweep'[32] of X and Y).

around the B—P bond illustrates this: the chemical shift changes from $\delta = -131$ (**38**) to $\delta = -288$ [TS, $PH_2(BH_2)$], and from $\delta = -17$ (**30**) to $\delta = -152$ [TS, $P(CH_3)_2(BH_2)$], respectively. This accompanies the loss of deshielding contributions attributed to the Lp(P), $\Delta\sigma(^{31}P)$(Lp(P)), from -131 (**38**) to -69 (TS of PH_2BH_2), and from -145 (**30**) to -65 [TS, $P(CH_3)_2(BH_2)$], respectively.[64]

In diborylphosphanes (**41**–**48**, Fig. 5), the phosphorus lone pair can conjugate to two BH_2 substituents, each of which has one empty p-AO. Consequently, the $P(BH_2)_2Y$ molecules have a characteristic 2π electron H_2B—P—BH_2 fragment. The three-center π bonding is responsible for the large $\sum \alpha$ value characterizing the reduced pyramidality[65] at phosphorus.[66] Increased pπ character of phosphorus bonding is reflected by $sp^{2.3}$ to $sp^{3.0}$ hybridization for $P(BH_2)_2Y$ (PH_3 is $sp^{2.1}$; Table 3). The P—B bond length is remarkably constant for Y = F to CH_3 (1.838 Å in **41** with Y = F, 1.833 Å in **42**, 1.834 Å in **43** and 1.834 Å in **44** with Y = CH_3). The B—P—B π system appears to have little interaction with π donor substituents.

$P(NH_2)_2Y$, $P(OH)_2Y$ and PF_2Y (group C)

In contrast to groups A and B (discussed above), the $\delta(^{31}P)$–$\sum EN$ slope for the PF_2Y set (filled squares in Fig. 13) is negative (-105 ppm per *EN* 'unit'). This 'inverse' relationship is less pronounced in the $P(OH)_2Y$ set (open circles in Fig. 13) and the $P(NH_2)_2Y$ set has a positive $\delta(^{31}P)$–$\sum EN$ slope (considerable scatter in both PX_2Y sets). Is the 'inverse' PF_2Y behavior related to any of the principle component analysis descriptors? The $\sum EN$, $\sum \alpha$ and ε_{LUMO} descriptors in Eqn (2) are not responsible (large deviations of 97 ppm for PF_2Me to -121 ppm for PF_3) between $\delta(^{31}P)_{PCA}$ and $\delta(^{31}P)$, Fig. 9). Reed and Schleyer[56] noted that negative hyperconjugation, NHC, was largest with fluorine substituents (e.g. in compounds with tricoordinate phosphorus). Consequently, the difference between the estimated [Eqn (2)] and the *ab initio* ^{31}P NMR chemical shifts, $\Delta\delta(^{31}P)$ (est., *ab initio*), was plotted (Fig. 14) against the extent of NHC, E_{nhc}, obtained by NBO analysis (see Computational Methods).

The correlation line (cc = 0.919) in Fig. 14 supports the conjecture that NHC is important. This 'local' correlation can be used to refine the NMR shift estimate for these molecules (Eqn (3), Table 5). The rmse of $\delta(^{31}P)$ from Eqn (3) vs $\delta(^{31}P)\}$ is small (20 ppm) and the agreement with experimental phosphorus NMR chemical shifts is reasonable (Table 5).

$$\delta(^{31}P) = -635 + 59.4 \sum EN + 1.87 \sum \alpha - 1746\varepsilon_{LUMO} - 5.62E_{nhc} \quad (3)$$

PX_2Y molecules with $\sum EN > 10$ (Fig. 14, '$PF_2^-BeH^+$,' **7**, excluded) comprise the PF_2Y subset, the $P(OH)_2Y$ set with Y = F, OH, NH_2 and $P(NH_2)_2F$. The extensive negative hyperconjugative interactions between the substituent lone pair [e.g. Lp(Y)] and the antibonding orbitals of another substituent [e.g. σ^*(PX)] appears to be responsible for the 'inverse' $\delta(^{31}P)$–$\sum EN$ relationship in these molecules. These negative hyperconjugative interactions also probably are responsible for the variation of the Lp(P) (Table 3) and P—F bond contributions to the phosphorus chemical shifts, $-\Delta\sigma(^{31}P)$(P—F): 105 (PF_3), 78 (PF_2Me) and 13 ($P(NH_2)_2F$), 0 (PMe_2F)).

PXYZ

We have also examined PXYZ molecules with three different 'simple first-row substituents', **65**–**120** (geometries in supplementary material). A plot of $\delta(^{31}P)$ against

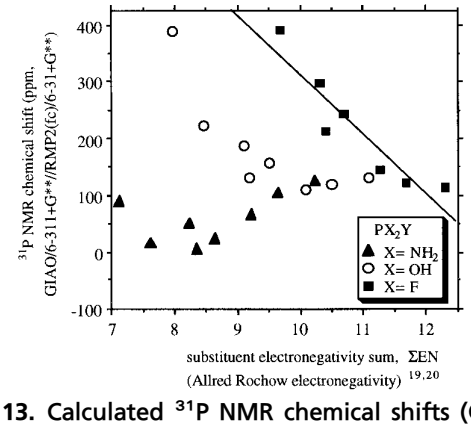

Figure 13. Calculated ^{31}P NMR chemical shifts (GIAO/6–311 + G**//RMP2(fc)/6–31 + G**) versus the substituent electronegativity sum, $\sum EN$ (Allred–Rochow electronegativity), for a subset (X = NH_2, OH, F and 'first-row sweep'[32] of Y) of the PX_2Y in Fig. 6 ('first-row sweep'[32] of X and Y). Correlation line (slope = -105 ppm per EN 'unit') for the PF_2Y molecules included.

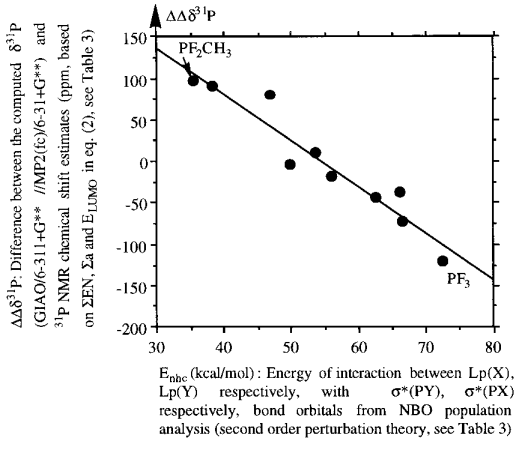

Figure 14. Difference between the computed $\delta(^{31}P)$ (GIAO/6–311 + G**//MP2(fc)/6–31 + G**) and ^{31}P NMR chemical shift estimates based on Eqn (2) versus E_{nhc} (energy of interaction between Lp(X), Lp(Y) respectively, and σ^*(PY), from NBO population analysis) for PX_2Y with $\sum EN > 10$ including the correlation line (cc = 0.919).

Table 5. Experimental[a–e,h,i], estimated[f] and *ab initio*[g] ^{31}P NMR chemical shifts of PX_2Y phosphanes with highly electronegative substituents ($\sum EN > 10$; X, Y = H, first-row substituents, numbering according to Fig. 4)

	PF_3 (1)	F_2POH (2)	F_2PNH_2 (3)	F_2PMe (4)	F_2PH (5)
Experimental	105.66[a] 97(l)[b]	(111)[c]	147.5[d]	250.7[e]	...
Estimate[f]	131	124	116	252	213
GIAO–G94[g]	112	121	146	244	211
	F_2PBH_2 (6)	$PF(OH)_2$ (9)	$P(OH)_3$ (10)	$P(OH)_2NH_2$ (11)	$PF(NH_2)_2$ (17)
Experimental	...	...	(141)[h]	(148)[i]	...
Estimate[f]	258	127	129	140	120
GIAO–G94[g]	296	130	119	109	126

[a] Gas-phase measurements with extrapolation to zero pressure value, Ref. 68.
[b] Ref. 69.
[c] $PF_2(OMe)$, Ref. 76.
[d] Ref. 70.
[e] Ref. 71.
[f] Estimate derived with Eqn (3): $\delta(^{31}P) = -635 + 59.4 \sum EN + 1.87 \sum \alpha - 1746\varepsilon_{LUMO} - 5.62E_{nhc}$; see text.
[g] GIAO[43]/6–311 + G**//RMP2(fc)/6–31 + G** from Table 3.
[h] $P(OMe)_3$, Ref. 77.
[i] $P(OMe)_2(NMe_2)$, Ref. 78.

$\sum EN$ (Fig. S-1, supplementary material) is similar to Fig. 6 and the $\delta(^{31}P)$–$\sum \alpha$ plot (Fig. S-2, supplementary material) is similar to Fig. 7. The 'inverse' $\delta(^{31}P)$–$\sum EN$ relationship for molecules with highly electronegative substituents is also found (see discussion of group **C** subsets of PX_2Y). Furthermore, the ^{31}P chemical shifts of the molecules of **65–120** which have less electronegative substituents than phosphorus (Li, BeH and BH_2) scatter considerably when plotted against $\sum EN$ (Fig. S-1, supplementary material). Application of the principle component analysis equation [Eqn (2)], only the $\sum EN$ and $\sum \alpha$ terms considered) performs similarly for **65–120** (rmse: 114 ppm; Fig. S-3, supplementary material) as for the PX_2Y set, **1–64** (rmse: 113 ppm; Fig. 9). Therefore, the PX_2Y set (discussed above) represents the behavior of the complete PXYZ set, **1–120**.

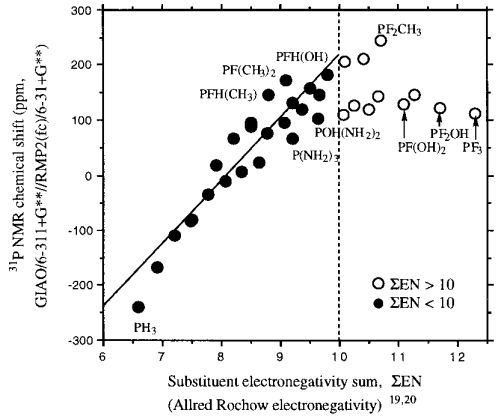

Figure 15. Calculated ^{31}P NMR chemical shifts [GIAO/6–311 + G**//RMP2(fc)/6–31 + G**] versus the substituent electronegativity sum, $\sum EN = EN(X) + EN(Y) + EN(Z)$, for PXYZ (X, Y, Z = H, CH_3, NH_2, OH and F, molecules with $\sum EN > 10$ excluded). Correlation line with slope 115 ppm per EN 'unit' (cc: 0.877).

Which part of the PXYZ subset has a 'normal' $\sum EN$ shift relationship? If the lithium, beryllium and boron derivatives and the molecules with $\sum EN > 10$ are omitted (this leaves the solid points in Fig. 15), the $\delta(^{31}P)$–$\sum EN$ relationship with cc = 0.877 is found. No solid point in Fig. 15 deviates by more than 70 ppm from the correlation line (deviations are 70 ppm for $PFHCH_3$, 63 for $PF(CH_3)_2$, −57 for $P(NH_2)_3$, −63 for (PH_3) and −64 for $POH(NH_2)_2$). The $\delta(^{31}P)$–$\sum EN$ slope of the correlation line (115 ppm per EN 'unit') is in reasonable agreement with the experimentally known slope for dimethylphosphane derivatives [146 ppm per EN 'unit', Fig. 2(c)].

CONCLUSIONS

Considerable scatter is found in all plots of calculated (GIAO/6–311 + G**//RMP2(fc)/6–31 + G**) $\delta(^{31}P)$ versus geometric (e.g. $\sum \alpha$, bond angle sum), energetic (e.g. energy of the HOMO) or electronic (sp^x, valence hybridization) descriptors considered for the complete set of PXYZ phosphanes with 'simple first-row substituents,' X, Y, Z: F, OH, NH_2, CH_3, BH_2, BeH, Li, H). The substituent electronegativity sum, $\sum EN$, is the main influence among various principle component analysis descriptors. In contrast to other PX_2Y sets, the PH_2Y subsets display the 'best' $\delta(^{31}P)$–$\sum EN$ relationships (cc = 0.955 and 0.853, respectively, upfield shift with decreasing EN(Y)[2.0]). The $\delta(^{31}P)$–$\sum EN$ 'low limit line' in Fig. 6 curves down for phosphanes with highly electronegative substituents ($\sum EN > 10$). We attribute

this behavior to negative hyperconjugation. Even the behavior of a selected set of PXYZ molecules with the H, CH_3, NH_2, OH and F substituents (derivatives with $\sum EN > 10$ excluded) is less than satisfactory: the $\delta(^{31}P)$–$\sum EN$ relationship has cc = 0.877 (Fig. 15).

SUPPLEMENTARY MATERIAL

Supplementary material is available from the authors: figures of the MP2(fc)/6–31G* geometries of molecules **65–120**; diagrams ($\delta(^{31}P)$ vs $\sum EN$, $\delta(^{31}P)$ vs $\sum \alpha$, and $\delta(^{31}P)$ (estimated) vs $\delta(^{31}P)$(*ab initio*)) for **65–120**; *ab initio* NMR results in NMR—SHARC format at http://www.ccc.uni-erlangen.de/sharc/; tables of $\delta(^{31}P)$ values derived with substituent shift increments from the literature (Refs 1, 2 and 16).

Acknowledgments

We thank Professor J. Hahn, Dr K. Karaghiosoff and Dr M. Kaupp for productive discussions and the Deutsche Forschungsgemeinschaft (DFG, Graduiertenkellog 'Phosphorchemie als Bindeglied verschiedener chemischer Disziplinen') for financial support.

REFERENCES

1. J. R. Van Wazer, C. F. Callis, J. N. Shoolery and R. C. Jones, *J. Am. Chem. Soc.* **78**, 5715 (1956).
2. R. A. Y. Jones and A. R. Katritzky, *Angew. Chem.* **74**, 60 (1962).
3. M. Baudler, U. M. Krause, J. Hahn and R. Riekehof-Böhmer, *Z. Anorg. Allg. Chem.* **543**, 35 (1986).
4. J. Emsley, R. Feeney and L. H. Sutcliffe, *High Resolution NMR Spectroscopy*, p. 1056. Pergamon, New York (1966).
5. S. G. Kleemann, E. Fluck, J. C. Tebby, A. W. G. Platt, Y. Leroux, R. Burgada, L. Maier and P. J. Diel, in *Handbook of Phosphorus-31 Nuclear Magnetic Resonance Data*, edited by J. Tebby, p. 49. CRC Press, Boca Raton, FL (1991).
6. S. O. Grim, W. McFarlane, and E. F. Davidoff, *J. Org. Chem.* **32**, 781 (1967).
7. H. Friebolin, *Basic One and Two Dimensional NMR Spectroscopy*, p. 48. VCH, New York (1991).
8. The large errors [160 (CF_4), 90 (CHF_3), 30 (CH_2F_2) and 10 ppm (CH_3F)] in $\delta(^{13}C)$ estimates obtained with the 70 ppm increment for C—F [based on $\delta(^{13}C)$ of CH_3F] can be reduced to deviations of 40, 0, −30 and −20 ppm, respectively, by using a 40 ppm C—F increment.
9. Mismatches of −23 to 24 ppm (11 examples, rmse 15 ppm; Refs 1, 37 and 69), −47 to 94 ppm (18 examples, rmse 36, Refs 2 and 37) and −134 to 25 ppm (65 examples, rmse 41 ppm, Refs 5 and 37) have been reported. Estimates based on a combination of $\delta(^{31}P)$ increments from Refs 1 and 21 compared with 72 experimental values give an rmse of 69 ppm; the largest deviations are 25 and −217 ppm for shift values between −240 and 244 ppm.
10. J. M. Foster and S. F. Boys, *Rev. Mod. Phys.* **32**, 300 (1960).
11. W. Kutzelnigg, U. Fleischer and M. Schindler, in *NMR Basic Principles and Progress*, Vol. 23, p. 234. Springer, Heidelberg (1990).
12. G. Rauhut and T. Clark, *J. Comput. Chem.* **14**, 503 (1993).
13. D. E. Rumelhart, G. E. Hinton and R. J. Williams, *Nature (London)* **323**, 533 (1986).
14. J. J. P. Stewart, *J. Comput. Chem.* **10**, 209 (1989).
15. A. R. v. Onciul, Dissertation, Erlangen-Nürnberg (1994).
16. J. Tebby (Ed.), *Handbook of Phosphorus-31 Nuclear Magnetic Resonance Data*. CRC Press, Boca Raton, FL (1991).
17. A 'descriptor' is a statistical term for factors which could be employed to estimate a property of interest.
18. D. R. Armstrong, P. G. Perkins and J. J. P. Stewart, *J. Chem. Soc., Perkin Trans. 2* 838 (1973).
19. A. L. Allred and E. Rochow, *J. Inorg. Nucl. Chem.* **5**, 264 (1958).
20. The substituent electronegativity[19] is that of the atom bonded to phosphorus.
21. L. Maier, P. J. Diel and J. C. Tebby, in *Handbook of Phosphorus-31 Nuclear Magnetic Resonance Data*, edited by J. Tebby, p. 121. CRC Press, Boca Raton, FL (1991).
22. L. R. Smith and J. L. Mills, *J. Am. Chem. Soc.* **98**, 3852 (1976).
23. J. Hahn, M. Baudler, C. Krüger and Y.-H. Tsay, *Z. Naturforsch., Teil B* **37**, 797 (1982).
24. The original increments are based on PMe_3 (INC(CH_3) = 0): INC(Et) = 14, INC(^{i}Pr) = 27, INC(^{t}Bu) = 41 [Ref. 21; L. Maier, *Helv. Chim. Acta* **49**, 1718 (1966); E. Fluck and J. Lorenz, *Z. Naturforsch., Teil B* **22**, 1095 (1967)]. The general equation [INX(alkyl) = 21 − $14n_\beta$ + $3n_\gamma$ with INC(CH_3) = 21 and INC(Ph) = 0 as reference] was published in Ref. 6. The ranking of the increments is similar to β-substituent effects for hydrocarbons: ^{13}C NMR shift increments for complex alkyl substituents can be generated with the equation $\delta(^{13}C) = -2.3 + 9.1n_\alpha + 9.4n_\beta - 2.5n_\gamma$ with n_α, n_β, n_γ = number of α-, β- and γ-alkyl substituents.[7] Oligophosphanes, P_nH_{n+2}, display large β-substituent effects on the chemical shift which can be described by the equation $\delta(^{31}P) = -215 + 22n_\alpha + 32n_\beta - 7n_\gamma$ (with n_α, n_β, n_γ = number of α-, β- and γ-substituents, largest error below 5 ppm; Ref. 3).
25. D. B. Chesnut and C. K. Foley, *J. Chem. Phys.* **85**, 2814 (1986).
26. D. G. Gorenstein, in *Handbook of Organophosphorus Chemistry*, edited by H. Engel, p. 441. CRC Press, Boca Raton, FL (1992).
27. K. R. Dixon, *Phosphorus to Bismuth in Multinuclear NMR*, J. Mason (Ed.), Chapt. 13, p. 369. Plenum Press, London (1987).
28. (a) Ref. 69 gives 97 ppm for the liquid phase; (b) recent gas-phase measurements[68] give 105.66 ppm.
29. F. Seel and K. Rudolph, *Z. Anorg. Allg. Chem.* **359**, 233 (1968).
30. GIAO/6–311 + G**//RMP2(fc)/6–31 + G* values from Table 3, Fig. 4.
31. M. Regitz and O. J. Scherer, *Multiple Bonds and Low Coordination in Phosphorus Chemistry*. Georg Thieme, Stuttgart (1990).
32. W. Hehre, L. Radom, P. v. R. Schleyer and J. A. Pople, *Ab Initio Molecular Orbital Theory*, p. 137. Wiley, New York (1986).
33. D. B. Chesnut and E. F. C. Byrd, *Heteroatom Chem.* **7**, 307 (1996).
34. A. E. Reed, L. A. Curtis and F. Weinhold, *Chem. Rev.* **88**, 899 (1988).
35. Our RMP2(fc)/6–31 + G** geometries are closest to the RMP2/6–311 + G** result reported for PFH_2 in a comprehensive method comparison by B. A. Smart and W. H. Rankin, *J. Chem. Soc., Chem. Commun.* 231 (1997).
36. L. Sachs, *Applied Statistics. A Handbook of Techniques*, 2 ed., p. 77. Springer, New York (1984).
37. The complete list of molecules considered and details of the statistical evaluation are provided in the supplementary material: (a) table of the experimental chemical shifts used to examine increment performance; (b) geometries of PXYZ phosphanes **65–120**.
38. M. J. Frisch, G. W. Trucks, H. B. Schlegel, P. M. W. Gill, B. G. Johnson, M. A. Robb, J. R. Cheeseman, T. Keith, G. A. Petersson, J. A. Montgomery, K. Raghavachari, M. A. Al-Laham, V. G. Zakrzewski, J. V. Ortiz, J. B. Foresman, J. Cioslowski, B. B. Stefanov, A. Nanayakkara, M. Challacombe, C. Y. Peng, P. Y. Ayala, W. Chen, M. W. Wong, J. L. Andres, E. S. Replogle, R. Gomperts, R. L. Martin, D. J. Fox, J. S. Binkley, D. J. Defrees, J. Baker, J. P. Stewart, M. Head-Gordon, C. Gonzalez and J. A. Pople, *Gaussian 94 (Revision C)*. Gaussian, Pittsburgh, PA (1995).
39. J. A. Pople, K. Raghvachari, H. B. Schlegel and J. S. Binkley, *Int. J. Quantum Chem.* **13**, 225 (1979).
40. D. B. Chesnut and D. W. Wright, *J. Comput. Chem.* **12**, 546 (1991).
41. A. Dransfeld and P. v. R. Schleyer, paper presented at the XIII International Conference on Phosphorus Chemistry, Jerusalem, 1995.
42. K. Wolinski, J. Hinton and P. Pulay, *J. Am. Chem. Soc.* **112**, 8251 (1990).
43. J. R. Cheeseman, G. W. Trucks, T. A. Keith and M. J. Frisch, *J. Chem. Phys.* **104**, 5497 (1996).
44. The change in the isotropic phosphorus shielding with the number of *d*-functions, *n*, in 6–311 + G(nd, p) is systematic for PH_3 (n = 1, 592.9; n = 2, 584.2; n = 3, 581.3), PMe_3 (n = 1, 433.8; n = 2, 419.3; n = 3, 413.6). However, the difference vanishes with increasing substituent electronegativity sum: PF_3 (n = 1, 240.8; n = 2, 240.6; n = 3, 238.7).
45. The phosphorus chemical shift [$\delta(^{31}P)$, with respect to 85% H_3PO_4] is related to the absolute magnetic shielding [$\sigma(^{31}P)$] by $\delta(^{31}P)(X) - \delta(^{31}P)(PH_3) = -[\sigma(X) - \sigma(PH_3)]$ with $\delta(^{31}P)(PH_3) = -240$ and $\sigma(PH_3)$ [GIAO/6–311 + G**//MP2(fc)/6–31 + G**] = 592.9 (see Table 3).
46. M. Bühl and P. v. R. Schleyer, *Inorg. Chem.* **30**, 3107 (1991).

47. H. Günther, *NMR-Spektroskopie: eine Einführung in der Protonenresonanz-Spektroskopie und ihre Anwendung in der Chemie*, 2nd ed., p. 9. Georg Thieme, Stuttgart (1983).
48. W. E. Lamb, *Phys. Rev.* **60**, 817 (1941).
49. R. K. Harris, *Nuclear Magnetic Resonance Spectroscopy: A Physicochemical View*. Wiley, New York (1986).
50. 'Quantization of magnetic dipolar energy in the field B_0 can readily be incorporated ... by the quantum number.'[49]
51. N. F. Ramsey, *Phys. Rev.* **78**, 699 (1950).
52. Ref. 43 and references cited therein. For semiempirical approximations, see I. Ando and G. A. Webb, *Theory of NMR Parameters*. Academic Press, London (1983).
53. The Larmor precession is an electromagnetic model in which 'quantization of the magnetic dipole energy [nuclear magnetic moment change] can be incorporated' to mimic the quantum mechanical (QM) effects. In contrast to molecular changes of magnetic moments which require QM treatment, the macroscopic change of magnetic moments in NMR pulse experiments is appropriately described by classical statistical physics. Furthermore, the macroscopic effective magnetic field at the position of the molecule, B_{cave}, is appropriately described by $B_{cave} = B_0 + \sum f(r)\chi(\text{neighbor})B_0$.
54. 'Each orbital contribution consists of three parts: $\sigma = \sigma^d + \sigma^{p_0} + \sigma^{p_1}$' (Ref. 11). In some approaches terms such as 'the contribution from the magnetic anisotropy of neighboring groups' and from 'the ring current effects in arenes' occur (see Ref. 7, p. 40).
55. E. D. Glendening, A. E. Reed, J. E. Carpenter and F. Weinhold, NAO population analysis program (1988).
56. A. Reed and P. v. R. Schleyer, *J. Am. Chem. Soc.* **109**, 7362 (1987).
57. U. Salzner and P. v. R. Schleyer, *J. Am. Chem. Soc.* **115**, 10231 (1993).
58. J. H. Letcher and J. R. Van Wazer, *J. Chem. Phys.* **44**, 815 (1966).
59. J. Pipek and P. G. Mezey, *J. Chem. Phys.* **90**, 4916 (1989).
60. T. D. Bouman and A. E. Hansen, *Chem. Phys. Lett.* **175**, 292 (1990).
61. The rmse [estimates with $\delta(^{31}P) = -390 + 59 \sum EN$ compared with *ab initio* results] for our complete set of PX_2Y with 'simple substituents' (Table 3) is 122 ppm.
62. P. v. R. Schleyer, *Pure Appl. Chem.* **55**, 355 (1983).
63. E. Kaufmann, T. Clark and P. v. R. Schleyer, *J. Am. Chem. Soc.* **106**, 1856 (1984).
64. Computation of $\delta(^{31}P)$ for the TS structures with the B—P bond length fixed to the value of the minimum differ by less than 1 ppm from the shift of the TS itself. Therefore, these $\Delta\sigma(^{31}P)(Lp(P))$ differences comparing the TS and the minimum are not due to the elongation of the B—P bond in the TS [1.954 Å (TS) and 1.862 Å (minimum) for PH_2BH_2 and 1.944 Å (TS) and 1.820 Å (minimum) for $P(CH_3)_2(BH_2)$].
65. T. P. Radhakrishnan and I. Agranat, *Struct. Chem.* **2**, 107 (1991).
66. M. B. Coolidge and W. T. Borden, *J. Am. Chem. Soc.* **112**, 1704 (1990).
67. H. Meier, in *Spektroskopische Methoden in der Organischen Chemie*, edited by M. Hesse, H. Meier and B. Zeeh, p. 222. Georg Thieme, New York (1984).
68. C. J. Jameson, A. De Dios and A. K. Jameson, *Chem. Phys. Lett.* **167**, 575 (1990).
69. H. S. Gutowsky, D. W. McCall and C. P. Slichter, *J. Chem. Phys.* **21**, 279 (1953).
70. D. E. J. Arnold and D. W. H. Rankin, *J. Chem. Soc., Dalton Trans.* 889 (1975).
71. G. S. Reddy and R. Schmutzler, *Inorg. Chem.* **6**, 823 (1967).
72. D. B. Chesnut and B. E. Rusiloski, *Chem. Phys.* **157**, 105 (1991).
73. U. Fleischer and W. Kutzelnigg, *Phosphorus Sulfur Silicon* **77**, 105 (1993).
74. H. Schäfer, G. Fritz and W. Hölderich, *Z. Anorg. Allg. Chem.* **428**, 222 (1977).
75. L. Riesel, D. Sturm, A. Nagel, S. Taudien, A. Beuster and A. Karwatzki, *Z. Anorg. Allg. Chem.* **542**, 157 (1986).
76. H. S. Gutowsky and D. W. McCall, *J. Chem. Phys.* **22**, 162 (1954).
77. V. Mark, C. H. Duncan, M. M. Crutchfield and J. R. Van Wazer (Eds), *Compilation of P31 NMR Data*, Vol. 5, p. 227. Interscience, New York (1967).
78. R. Burgada, *Bull. Soc. Chim. Fr.* 137 (1971).
79. K. M. Abraham and J. R. Van Wazer, *J. Inorg. Nucl. Chem.* **37**, 541 (1974).
80. L. F. Centofanti, *Inorg. Chem.* **12**, 1131 (1976).
81. Limitation to isolated phosphane molecules with 'simple' substituents and 'frozen' geometries leaves steric, electronic (e.g. β-substituent effects), temperature and solvent effects unconsidered. Therefore, comparison of our computed $\delta(^{31}P)$ with experimental data of related phosphanes is likely to deviate (due more to the neglected effects than to insufficiency of the theoretical treatment).